PERGAMON

Chemosphere 46 (2002) 797–807

CHEMOSPHERE

www.elsevier.com/locate/chemosphere

Kinetics of phenol and chlorophenol utilization by *Acinetobacter* species

Oliver J. Hao [a,*], Michael H. Kim [b], Eric A. Seagren [a], Hyunook Kim [c]

[a] *Department of Civil and Environmental Engineering, University of Maryland, College Park, MD 20742, USA*
[b] *Geo-Centers, Inc., P.O. Box 68, Aberdeen Proving Ground, MD 21010, USA*
[c] *Agricultural Research Service, Animal Waste & Byproduct Laboratory, Beltsville, MD 20705, USA*

Received 19 April 2001; received in revised form 7 August 2001; accepted 13 August 2001

Abstract

Although microbial transformations via cometabolism have been widely observed, the few available kinetic models of cometabolism have not adequately addressed the case of inhibition from both the growth and nongrowth substrates. The present study investigated the degradation kinetics of self-inhibitory growth (phenol) and nongrowth (4-chlorophenol, 4-CP) substrates, present individually and in combination. Specifically, batch experiments were performed using an *Acinetobacter* isolate growing on phenol alone and with 4-CP present. In addition, batch experiments were also performed to evaluate the transformation of 4-CP by resting, phenol-induced *Acinetobacter* cultures. The Haldane kinetic model adequately predicted the biodegradation of phenol alone, although a slight discrepancy was noted in cases of higher initial phenol concentrations. Similarly, a Haldane model for substrate utilization was also able to describe the trends in 4-CP transformation by the resting cell cultures. The 4-CP transformation by the *Acinetobacter* species growing on phenol was modeled using a competitive kinetic model of cometabolism, which included growth and nongrowth substrate inhibition and cross-inhibition terms. Excellent agreement was obtained between the model predictions using experimentally estimated parameter values and the experimental data for the synchronous disappearance of phenol and 4-CP.

Keywords: *Acinetobacter*; Phenol; 4-chlorophenol; Cometabolism; Kinetics; Inhibition

1. Introduction

The bacterial specific growth rate is often described using Monod kinetics. However, higher substrate concentrations may become inhibitory to microbial growth. For example, phenol at sufficiently high concentrations has been observed to exhibit an inhibitory effect on pure microbial cultures (e.g., Hill and Robinson, 1975; Yang and Humphrey, 1975) and activated sludge systems (e.g., Pawlowsky and Howell, 1973; D'Adamo et al., 1984). Evaluation of substrate inhibition becomes an important consideration in the treatment of toxic compounds (e.g., phenol) in engineered systems such as activated sludge processes. Although the substrate inhibition in a single enzyme-catalyzed reaction has been mechanistically well characterized, the same cannot be stated in regard to the substrate inhibition mechanism in a microbial growth system. Substrate inhibition of microorganisms has been partially attributed to many mechanisms that affect the overall microbial growth process (Edwards, 1970).

Several mathematical models have been developed to quantify inhibitory effects of toxic substrates on microbial growth kinetics (e.g., Edwards, 1970). Most of these equations have been adopted from models of the substrate inhibition of enzymatic reactions, and involve a

* Corresponding author. Tel.: +1-301-405-1961; fax: +1-301-405-2585.
E-mail address: ojh1@eng.umd.edu (O.J. Hao).

0045-6535/02/$ - see front matter
PII: S0045-6535(01)00182-5

common substrate inhibition term (K_{11}). The Haldane equation is one of the most commonly used models for describing the growth inhibition kinetics of microorganisms (Andrews, 1968):

$$\mu = \frac{\mu_{max} S_1}{K_1 + S_1 + (S_1^2/K_{11})}, \quad (1)$$

where S_1 and K_1 are the substrate concentration and the half-saturation coefficient, respectively. Because phenolic compounds are present in many industrial wastes, and *Acinetobacter* species play a significant role in activated sludge processes (e.g., Kim et al., 1997), the applicability of the Haldane equation for phenol degradation by this particular bacterial species is of interest.

Microbial cometabolism involves the transformation of a secondary substrate (nongrowth substrate) in the presence of the primary substrate (growth substrate). Often, the nongrowth substrate (e.g., chlorophenol, CP) itself exerts an inhibitory effect (K_{22}) on its own transformation in the presence of the growth substrate (e.g., phenol). Despite the widespread occurrence of microbial cometabolism, the few existing kinetic models of cometabolism have not adequately addressed the case of inhibition from both growth and nongrowth substrates. For example, in their modeling analyses of the degradation of phenol and 4-CP together, Sáez and Rittmann (1993) only included the K_{11} term for the self-inhibitory primary substrate, phenol. Recently, the inhibition terms for both substrates, as well cross-inhibitory terms between the interaction of growth- and nongrowth-enzyme complexes, have been discussed (Kim and Hao, 1999). Specifically, the observed simultaneous disappearance of both growth (phenol) and nongrowth substrates (4- or 3-CP), or the incomplete transformation of 4- or 3-CP, in the presence of phenol was explained based on the energy availability. In another study, Loh and Yu (2000) investigated the kinetics of a nongrowth substrate carbazole by a *Pseudomonas putida* strain, in the presence of sodium salicylate, a self-inhibitory growth substrate. Growth on sodium salicylate alone was described using Haldane kinetics. When both carbazole and sodium salicylate were present, carbazole inhibited its own degradation, as described by Haldane kinetics, as well as causing a greater inhibition of sodium salicylate degradation than the self-inhibition of sodium salicylate.

The main goal of this paper is to investigate the biodegradation kinetics of inhibitory growth and nongrowth substrates, present individually and in combination. Specifically, the objectives of the present study were to: (1) characterize the substrate inhibition at higher phenol concentrations by an isolated *Acinetobacter* strain, (2) describe kinetics of 4-CP transformation under resting cell conditions, and (3) validate an inhibition model by the growth (phenol) and nongrowth (4-CP) substrates using parameters estimated from phenol utilization tests alone, 4-CP transformation by *Acinetobacter* resting cells, and phenol/4-CP degradation data.

2. Materials and methods

2.1. Acinetobacter isolate

The selected *Acinetobacter* strain was isolated from activated sludge and identified as the genospecies complex 1-2-3 according to the classification proposed by Bouvet and Grimont (1986). This isolate was able to grow aerobically on phenol, but not 4-CP. However, phenol-grown cells readily degraded 4-CP under aerobic conditions. Additional characteristics of the *Acinetobacter* isolate, and details on its cometabolic degradation of 4-CP, are presented in Kim and Hao (1999).

2.2. Phenol degradation

For each batch experiment, autoclaved basal medium with phenol concentrations varying from 60 to 350 mg/l was added to a reactor (MultiGen, New Brunswick Scientific, 1 l of working volume). A detailed description of the basal medium composition is available in Kim and Hao (1999). Air was supplied by a built-in compressor and passed through a sterilized filter. Mixing was provided at 300 rpm, and a constant temperature of 30 °C was maintained. During the period of batch growth, samples were periodically taken for optical density analyses. Immediately after measurements of optical density, samples of suspended culture were centrifuged (Beckman GPR) at 3800 rpm for 15 min at 4 °C, filtered through glass fiber (Whatman GF/C) and 0.45 μm membrane (Gellman, GN-6) filters and stored at 4 °C for later analyses of phenol, 4-CP, and chemical oxygen demand (COD). The details of the analytical methods used for optical density measurements, phenol and 4-CP analyses by gas chromatography (GC), and COD are described in Kim and Hao (1999). A calibration curve was prepared between optical density and dry suspended solids. The same procedures were also followed in batch growth experiments using a mixture of phenol and 4-CP.

2.3. Resting cell experiments

Resting cell cultures of the *Acinetobacter* isolate were prepared after growth in a batch reactor (1 l) on basal medium containing 300 mg/l phenol. When cell growth neared the end of the exponential stage, as monitored by measurements of optical density, the reactor was dis-

mantled and known volumes of suspended culture were placed in tubes, centrifuged, washed with a saline solution, and recentrifuged. The concentrated cell pellet was mixed in a flask with 100 ml of a freshly prepared basal medium solution containing known 4-CP concentrations (10–75 mg/l). Samples were taken immediately after the mixing for 4-CP measurements. The mixtures were then incubated in a rotary shaker at 30 °C. Thereafter, culture samples (5 ml) were periodically taken, filtered through glass fiber and membrane filters, and stored at 4 °C for GC analyses of 4-CP.

3. Results and discussion

3.1. Phenol degradation

The results (phenol concentration and cell biomass) of phenol degradation tests for initial nominal phenol concentrations of 200 and 300 mg/l are shown in Figs. 1(a) and (b), respectively. Several duplicate runs were conducted and the reproducibility was reasonable. The rate of phenol utilization always increased as time progressed, a clear indication of the reduced inhibitory effect at lower phenol concentrations. This is also evident in the semi-log plot of Fig. 2. The initial specific growth rate, μ_i, of 0.45 h^{-1} immediately after inoculation was less than the observed maximum specific growth rate, μ_{max}, estimated from the upper portion of the growth curves prior to the stationary phase. The maximum specific growth rates for all batch experiments performed at 30 °C ranged from 0.80 to 0.85 h^{-1} (Table 1), with a mean value of 0.83 h^{-1}. As the initial phenol concentration increased, however, much lower values of the initial specific growth rates were obtained; a phenomenon solely due to substrate inhibition. Conversely, at the low initial phenol concentrations, the μ_i is close to the μ_{max}, e.g., they are 0.73 and 0.82 h^{-1}, respectively, at an initial nominal phenol concentration of 60 mg/l.

Biomass concentrations at the end of each batch run always abruptly increased even after phenol was completely utilized (Fig. 1(b)). Similar observations have also reported for the growth of *Pseudomonas* strains with phenol (Sáez and Rittmann, 1993) and with toluene, xylene or benzene (Chang et al., 1993). Transformation of various intra cellular metabolites that lag behind the phenol utilization rate might have contributed to the observed growth of *Acinetobacter* in the absence of phenol toward the end of each batch culture period (Allsop et al., 1993).

A typical example of a time-independent plot of biomass concentration versus residual phenol concentration is shown in Fig. 3, for an experiment with an initial nominal phenol concentration of 200 mg/l.

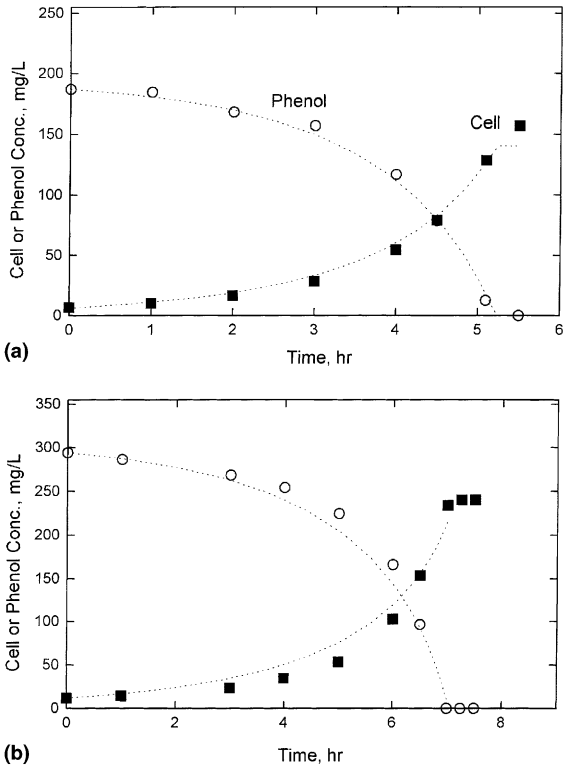

Fig. 1. Simulated and observed growth results of phenol degradation: (a) initial nominal phenol concentration of 200 mg/l, and (b) 300 mg/l.

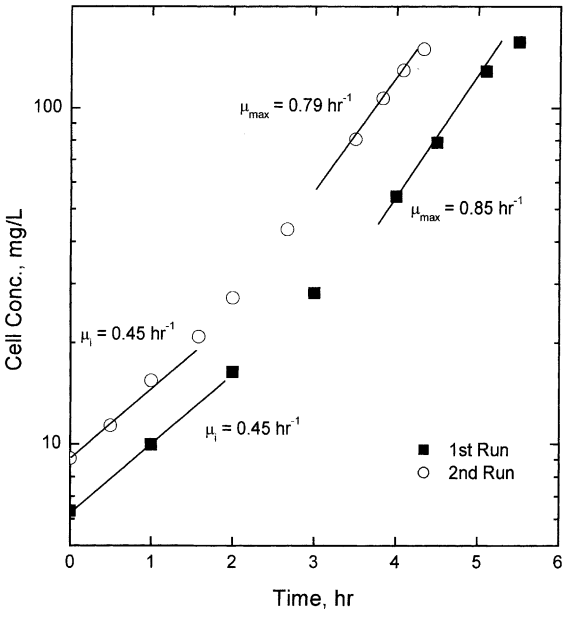

Fig. 2. Maximum growth rate estimation for initial nominal phenol concentration of 200 mg/l.

Table 1
Maximum growth rates, growth yield and inhibition constants of phenol utilization by an *Acinetobacter* species isolate at 30 °C

Initial phenol concentration (nominal), mg/l	Maximum specific growth rate, μ_{max}, h^{-1}	Yield constant, Y_m, mg cell/mg phenol	Inhibition constant, K_{I1}, mg/l
60	0.85	0.72	–
120	0.82	0.72	315
200	0.85	0.69	311
250	0.81	0.73	238
300	0.83	0.73	201
350	0.80	0.70	188
Mean	0.83	0.72	–

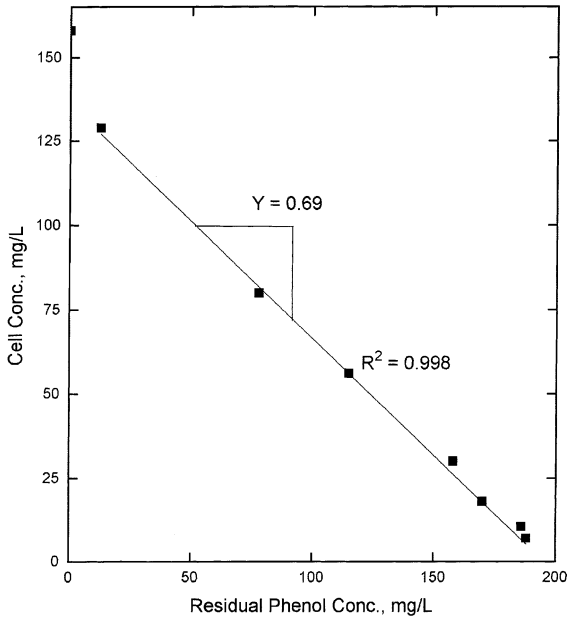

Fig. 3. Growth yield determination for initial nominal phenol concentration of 200 mg/l.

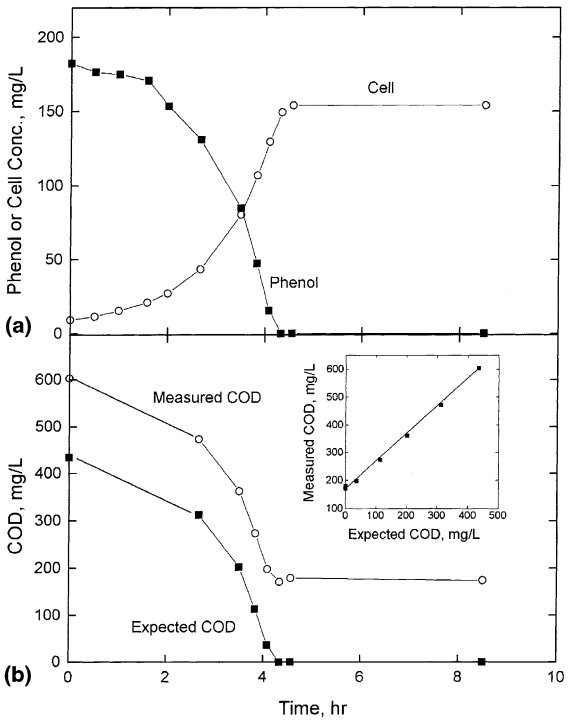

Fig. 4. COD measurement at initial nominal phenol concentration of 200 mg/l.

The biomass and phenol concentrations were linearly related for most of the active growth phase. The implication of this observation is that, despite the substrate inhibition, the yield coefficient is relatively constant. Coefficients of correlation for all experiments were above 0.99 with a mean yield (Y_m) value of 0.72 mg cell biomass/mg phenol utilized during the active growth period (Table 1). The relatively high growth yield value can be attributed to not only the high metabolic efficiency of *Acinetobacter*, but also to the high carbon/oxygen ratio in phenol. For instance, a lower growth yield value of 0.51 was reported for other *Acinetobacter* spp. growing on the more oxidized substrate acetate, which has a lower carbon/oxygen ratio (Du Preez et al., 1981). Nevertheless, the determined growth yield value was within the range of values (0.52–1.24) from other pure culture studies with phenol (e.g., Yang and Humphrey, 1975; Hill and Robinson, 1975; D'Adamo et al., 1984; Sáez and Rittmann, 1993).

The dissolved COD data (Fig. 4) indicate that phenol and/or intermediate metabolite leakage is not evident during the batch growth period of *Acinetobacter*. A 1:1 linear relationship was obtained between the expected COD due to the remaining phenol concentration (2.34 mg COD/mg phenol, as compared to the theoretical value of 2.38) and the measured COD values (insert in Fig. 4(b)). The measured COD was, however, always above the expected COD. This consistent difference can be attributed to the nitrilotriacetic acid used in the basal medium.

3.2. Substrate inhibition model

The following coupled equations for the phenol substrate utilization and the overall growth rates were used for model simulation:

$$\frac{dS_1}{dt} = \frac{-k_1 X S_1}{K_1 + S_1 + (S_1^2/K_{11})} \tag{2}$$

and

$$\frac{dX}{dt} = Y_m\left(\frac{-dS_1}{dt}\right) bX, \tag{3}$$

where k_1 is the maximum specific phenol utilization rate, mg/mg h, X is the biomass concentration, mg/l, and b is the decay coefficient, h^{-1}. Because the growth yield was constant (0.72 mg biomass/mg phenol utilized) and the decay coefficient ($b = 0.05\ d^{-1}$, not shown) could be neglected, Eq. (3) was integrated to yield the following linear equation:

$$X = X_0 + Y_m(S_{10} S_1), \tag{4}$$

where X_0 and S_{10} are initial biomass and substrate concentrations, respectively. Also, the maximum substrate utilization rate is related to the specific maximum growth rate as follows:

$$k_1 = \frac{\mu_{max}}{Y_m}. \tag{5}$$

Hence, the maximum phenol utilization rate was estimated to be 1.2 mg phenol/mg biomass h using the previously estimated μ_{max} and Y_m.

As a result, the number of fitting parameters for Eqs. (2) and (3) was reduced to two (i.e., K_1 and K_{11}), which were estimated by applying a dynamic nonlinear numerical fitting routine that used a steepest descent gradient method. The half saturation constant (K_1) was determined by using the data from the lowest initial phenol concentration batch experiment (60 mg/l), and several different initial K_1 values used for the estimation resulted in the same final estimate of 1.5 mg/l. Hence, the two values $k_1 = 1.2$ mg phenol/mg biomass h and $K_1 = 1.5$ mg/l were subsequently used in the estimation of inhibition constants for other phenol concentrations. The estimated K_{11} values are given in Table 1.

The consistently small magnitude of K_1 values (<1–2.4 mg/l) for all the pure culture studies (e.g., Yang and Humphrey, 1975; Hill and Robinson, 1975; D'Adamo et al., 1984; Sáez and Rittmann, 1993) indicate that for microbial species utilizing phenol, the maximum growth rate could be attained immediately, if substrate inhibition has not been a factor. However, a certain degree of substrate inhibition as reflected by the magnitude of the inhibition constant delays the attainment of the maximum growth rate. As compared to other pure culture studies (K_{11} values ranging 36–470 mg/l), phenol exerted a mild substrate inhibition on the *Acinetobacter* species used in this study (K_{11} values ranging 188–315 mg/l). A decreasing trend in K_{11} values was observed with increasing initial phenol concentrations (Table 1). The opposite results have been reported for the batch growth of *Pseudomonas* spp. (Sáez and Rittmann, 1993), i.e., increased values of K_{11} at higher initial phenol concentrations. Inspection of the Haldane equation, however, indicates that, if higher phenol concentrations exert more toxic effects, the value of K_{11} should decrease as shown in this study. Okaygun et al. (1992) have reported the same decreasing trend of K_{11} for activated sludges (predominantly *Pseudomonas* spp. and *Klebsiella* spp.) fed consecutively with pulse phenol loadings. They proposed an inhibition factor (γ) to explain the decreased K_{11} values such that the observed inhibition constant (K_{11}^{obs}) was related to the maximum inhibition constant (K_{11}^{m}) as follows:

$$K_{11}^{obs} = \frac{K_{11}^{m}}{\gamma}. \tag{6}$$

However, no such clear relationship was evident in this study.

The predicted values for both cell and substrate concentrations obtained by numerically solving Eqs. (2) and (3) and using the determined kinetic values matched the observed values well (dashed lines in Figs. 1(a) and (b)). A slight discrepancy, however, was noted in the cases of higher initial phenol concentrations. Predictive discrepancy of the Haldane equation in general can be best demonstrated by examining instantaneous specific growth rates under substrate inhibition conditions. The simulation results for cell concentration are plotted in a semi-log scale in Fig. 5 to compare with those of the actual growth data. Qualitatively, the simulation results indicate that there exists a threshold substrate concentration above which the instantaneous specific growth rate will be constant (i.e., the linear relationship is manifested in the early phase of simulated growth in Fig. 5). When the substrate concentration is reduced below the threshold limit, the instantaneous specific growth rate begins to increase to approach the maximum growth rate. In other words, the greatest change in instantaneous specific growth rates is always evident toward the end of the batch growth period. Similar results of the maximum instantaneous growth rate at the end of exponential growth were also obtained by using other substrate inhibition kinetic equations proposed by Edwards (1970).

On the contrary, the substrate-inhibited growth data in this study indicated that the substrate inhibition was apparently reduced from the very beginning of the growth, as evident by increases in the instantaneous specific growth rates in the earlier stage of the growth.

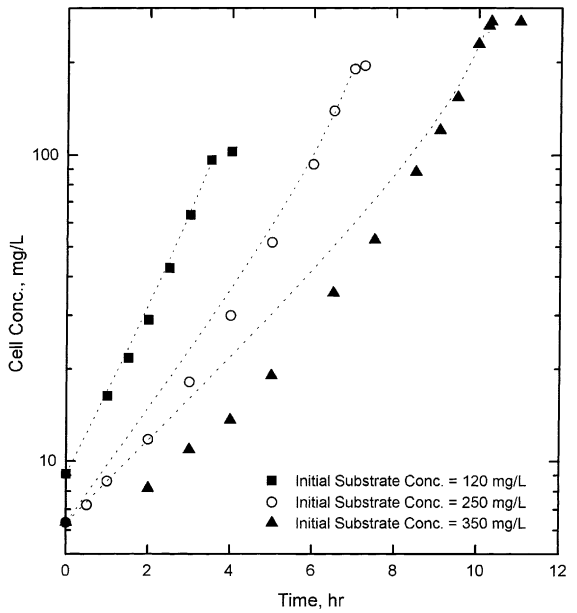

Fig. 5. Variation of specific growth rates due to phenol inhibition.

The instantaneous specific growth rate continued to increase from the time of inoculation, eventually approaching the maximum growth rate. The experimentally observed pattern of ever-increasing changes in the maximum growth rate in the early phase of the growth is expected because the reduced substrate concentration exerts a lesser inhibition on the growth. The observations of ever-increasing rates in the present study, are substantiated by other substrate-inhibition growth data, although not explicitly mentioned by the authors, e.g., the substrate inhibition in the growth of *Pseudomonas putida* ATCC 17484 on phenol (Hill and Robinson, 1975), growth of phenol-acclimated activated sludges on phenol (Rozich et al., 1985), and growth of both *Acinetobacter* and *Pseudomonas* spp. on benzoate (D'Aquino et al., 1988).

The error between the experimental and simulation growth results becomes insignificant as the initial phenol concentration is lowered (Fig. 5). This is expected because higher phenol concentrations would exert a higher substrate inhibition. The inadequacy of the Haldane substrate inhibition kinetics is apparent at higher substrate concentrations in which the gradual increase of instantaneous growth rate could not be accommodated. This inadequacy could also explain some inconsistencies reported in the literature. For instance, the Haldane substrate inhibition kinetic parameters obtained from batch growth data (i.e., high substrate concentrations) tend to overpredict the steady-state substrate concentrations (Rozich and Gaudy, 1985). On the other hand, the Haldane substrate kinetic parameters obtained from continuous culture steady-state growth data (i.e., low substrate concentrations) represent the steady-state growth data well (Yang and Humphrey, 1975). However, Haldane substrate inhibition kinetic models under dynamic conditions (e.g., increase in the feed substrate concentration) are severely limited in their predictability (Allsop et al., 1993).

The need for better understanding of substrate inhibition kinetic models is apparent. In particular, the gradual lessening of substrate inhibition as the substrate concentration decreases warrants a further evaluation in substrate inhibition kinetic models. A descriptive structured model has been suggested in which the substrate uptake rate is no longer a limiting factor, but rather the accumulation of unidentified intracellular intermediates is proposed to account for substrate inhibition (Allsop et al., 1993). However, the structured model approach would require greater effort in terms of estimation of an increased number of parameters and identification of suitable variables.

3.3. Resting cell experiments

The likely involvement of oxygenase-mediated reactions for transformation of 4-CP by phenol-grown *Acinetobacter* cells is demonstrated by the experimental results shown in Fig. 6. After the phenol was consumed (initial nominal concentration 250 mg/l) and the cell biomass concentration had leveled off, the batch reactor was purged with N_2 gas to create anaerobic conditions. One hour after N_2 purging was begun, 4-CP was added

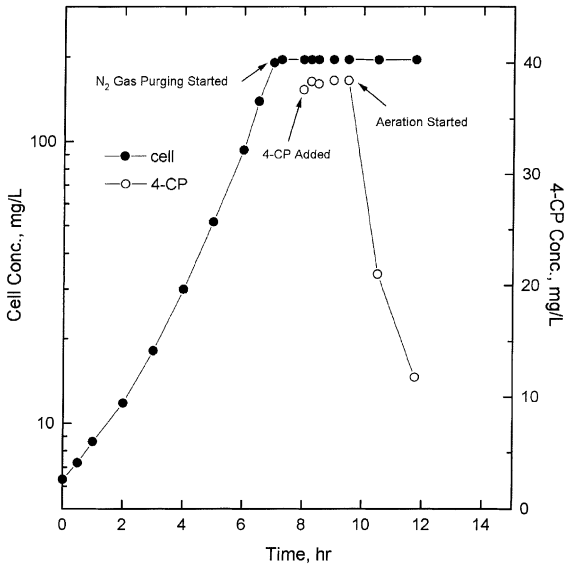

Fig. 6. Growth of *Acinetobacter* on phenol and aeration effect on 4-CP degradation (initial nominal phenol concentration = 250 mg/l).

at a nominal concentration of 40 mg/l. The concentration of 4-CP remained essentially the same after a 2 h anaerobic incubation period, but 4-CP was readily transformed when aeration was resumed. The involvement of the oxygenase enzymes for phenol oxidation in the observed 4-CP cometabolic transformation was further demonstrated by experiments (not shown) in which acetate grown cells were unable to transform 4-CP.

Resting cell transformation experiments were performed in two experimental arrays: (1) constant initial cell concentration with varying initial 4-CP concentration (Fig. 7(a)), and (2) constant initial 4-CP concentration with varying initial cell biomass concentrations (Fig. 7(b)). Three characteristics were evident in all of these batch experiments. The first characteristic was that the concentration of 4-CP was immediately reduced to a lower level (referring to 4-CP reduction between $t = 0$ and when the first sample could be taken at $t = 1/2$ min in Fig. 7). The amount of 4-CP immediately reduced during the initial sampling period (1/2 min) was proportional to the initial amount of cell biomass used (Fig. 8(a)). On the other hand, the different concentrations of 4-CP at a constant culture density of 182 mg/l only showed a relatively constant initial 4-CP reduction of 2 mg/l (Fig. 8(b)). Polnisch et al. (1992) have also reported the immediate 4-CP reduction by phenol-assimilating resting cells of yeast *Candida maltosa* and ascribed it to absorption onto cell surface. However, the exact reason(s) is unclear. Further study is needed to clarify the immediate reduction in concentration of chlorinated phenols by resting cells capable of cometabolism.

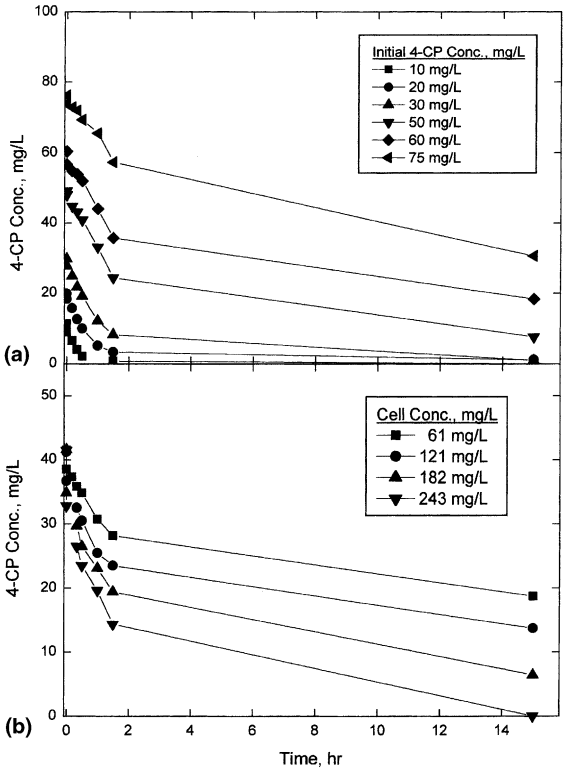

Fig. 7. Effect of initial 4-CP and cell concentrations on transformation of 4-CP by resting cells: (a) initial cell concentration = 182 mg/l, with variable initial 4-CP concentrations; and (b) initial 4-CP concentration = 40 mg/l, with variable initial cell concentrations.

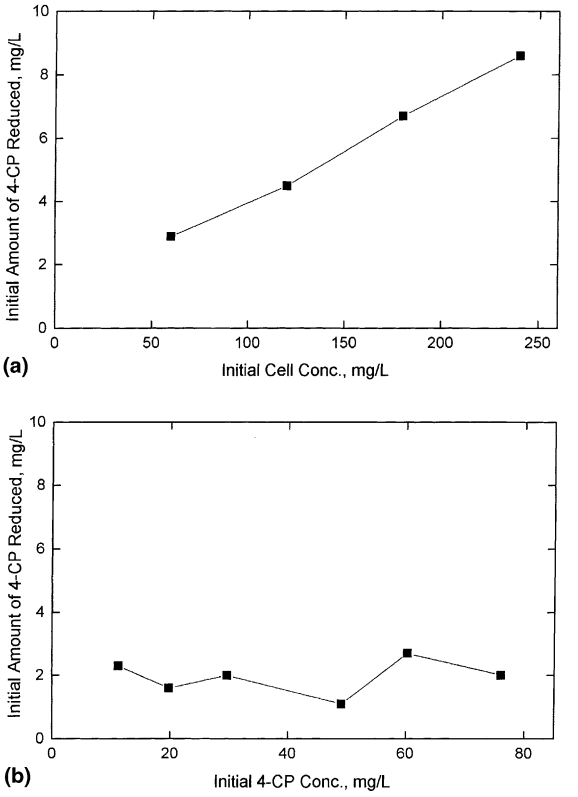

Fig. 8. Effect of initial cell (a) and 4-CP concentrations (b) on the amount of 4-CP reduced.

Secondly, resting cell cultures of *Acinetobacter* showed a residual amount of 4-CP in most of the experiments after 15 h, indicating a finite transformation capacity for 4-CP. The residual amount of 4-CP was higher for those experiments with higher initial amounts of 4-CP (or a lower amount of cells). This initial 4-CP (or cell) concentration-dependent effect on the extent of residual 4-CP concentration implies that the depletion of cell internal energy might be responsible for the observed finite transformation capacity by resting cells of *Acinetobacter*.

The finite transformation capacity by resting cells has also been attributed to product toxicity, e.g., epoxide formation in TCE transformation (Fox et al., 1990;

Folsom et al., 1990; Oldenhuis et al., 1991). However, no product toxicity was associated with 4-CP transformation products for the growth of *Acinetobacter* species in the presence of phenol and 4-CP (Kim and Hao, 1999). This suggests that the finite 4-CP transformation capacity exhibited by resting cells of *Acinetobacter* species in this study could mainly be attributed to the limited amount of reductant supply during endogenous cell decay. Likewise, for other oxygenase systems that do not show product toxicity, the requirement of an electron donor cofactor could also be the critical limiting factor. However, for many resting cell transformation systems that show product toxicity, both limited reductant supply and product toxicity contribute to the finite transformation capacity of resting cells. How these two factors interact to affect the finite transformation capacity of resting cells is not clear (Alvarez-Cohen and McCarty, 1991).

Third, after the initial 4-CP reduction, the 4-CP decreased linearly (Fig. 7), but with reduced initial rates at higher initial 4-CP concentrations (Fig. 7(a)). The decreased 4-CP transformation rate with higher initial 4-CP concentration implies that 4-CP acts as an inhibitor. Therefore, the Haldane substrate inhibition model was used to characterize the 4-CP inhibition on its own transformation by resting cells of *Acinetobacter*. Because the 4-CP transformation is not coupled to the cell growth, only the substrate utilization term analogous to enzyme substrate inhibition kinetics is required to describe the kinetics of 4-CP transformation as follows:

$$v = \frac{dS_2}{dt} = \frac{k_2 X}{1 + (K_2/S_2) + (S_2/K_{22})}, \tag{7}$$

where S_2 is the 4-CP concentration, mg/l, k_2 is the maximum specific 4-CP transformation rate, mg 4-CP/mg cell h, K_2 is the half saturation coefficient for 4-CP, mg/l, and K_{22} is the inhibition constant, mg/l. In order to estimate the k_2 value, the specific initial 4-CP transformation rates were plotted against the initial cell concentration (Fig. 9). By extrapolating the linear line, the k_2 value of 0.15 mg 4-CP/mg cell h was determined.

At high S_2 concentrations, Eq. (7) is simplified as:

$$\frac{1}{v} = \frac{1}{k_2 X} + \frac{S_2}{K_{22} k_2 X}. \tag{8}$$

Plotting the inverse of the initial 4-CP transformation rate versus initial 4-CP concentrations yields a straight line at high 4-CP concentrations with a slope of 6.3×10^{-4} h/(mg 4-CP/l)^2, which represent $1/K_{22} \cdot k_2 \cdot X_0$ (not shown). Thus, a K_{22} value of 60 mg 4-CP/l was determined from the previously estimated k_2 value of 0.15 mg 4-CP/mg cell h and the initial cell concentration of 182 mg/l; the same value is also obtained from the x-intercept of the $1/v$ versus S_2 plot.

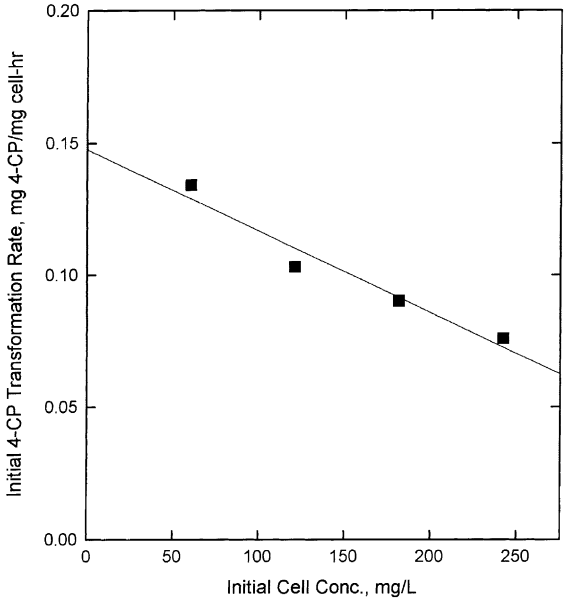

Fig. 9. k_2 Determination from the specific initial 4-CP transformation rates.

For comparison, the modeled and actual initial 4-CP transformation rates are shown in Fig. 10. Although the model prediction captures the general trends in the data, the magnitude of the predictions for the transformation rate do not match the data well. One possible explanation for this is a problem with one or more of the model parameter estimates. For example, the observed immediate reduction of 4-CP concentration upon contact with the resting cells of *Acinetobacter* could be due to an increased affinity of 4-CP for phenol-induced enzymes, in particular, the oxygenases involved in the initial co-oxidation of 4-CP. Because an electrophilic-type mechanism is speculated to be operative in oxygenase activities (Gibson, 1968; Hamilton, 1974; Fox et al., 1990), both the maximum transformation rate and affinity constant are significantly influenced by the substituent group on the cometabolite. In particular, the substituent groups significantly impact the transformation of substituted catechols, because the ring cleavage reaction is usually a limiting factor (Knackmuss and Helwig, 1978). Based on the results obtained by Dorn and Knackmuss (1978) using 1,2-dioxygenases, it is expected that the presence of an electron-withdrawing group (e.g., halogenated catechols) will reduce the maximum velocity and increase the affinity of catechol. Consistent with these findings, the estimated maximum specific rate value of $k_2 = 0.15$ mg 4-CP/mg cell h is less than $k_1 = 1.2$ mg phenol/mg cell h. Thus, a K_2 value of 0.15 mg/l for 4-CP by resting cells of *Acinetobacter* was estimated which was less than the K_1 value of 1.5 mg/l for phenol.

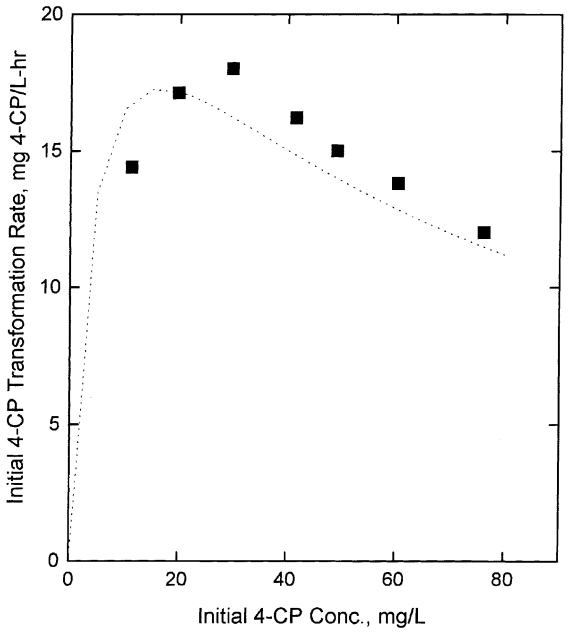

Fig. 10. Simulated and determined initial 4-CP transformation rates.

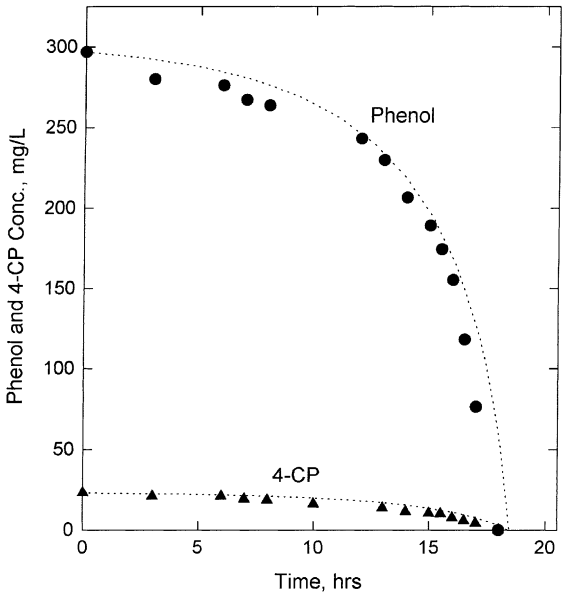

Fig. 11. Experimental data and model simulations for phenol and 4-CP degradation at an initial phenol:4-CP ratio of 300:25 mg/l.

The fact that K_2 actually decreased implies a short time to attain k_2, possibly causing the observed immediate 4-CP reduction, because the substrate had to bind to intracellular enzymes (e.g., oxygenases) before the transformation could proceed. This explanation is supported by the observation that the amount of 4-CP that disappeared is correlated with the initial amount of biomass present, not the initial 4-CP concentrations (Fig. 8).

3.4. 4-CP cometabolic transformation

A typical pattern for 4-CP transformation by the *Acinetobacter* isolate growing on phenol is shown in Fig. 11. Synchronous 4-CP and phenol utilization (e.g., Fig. 11) was observed when the initial phenol:4-CP concentration ratio was sufficiently high ($\geqslant$ 200:50 mg/l). Those runs resulting in the synchronous phenol utilization and 4-CP transformation indicated that sufficient energy from phenol utilization was available. On the other hand, the 4-CP transformation data with the initial phenol concentration lower than 200 mg/l (initial nominal 4-CP concentration = 50 mg/l) resulted in the incomplete 4-CP transformation (Kim and Hao, 1999). The focus here is on the 4-CP transformation data with initial phenol concentrations sufficient to result in the complete 4-CP transformation.

The 4-CP transformation in the presence of phenol was modeled based on the following equations, which are written in terms of the respective maximum rate constants (k_1, k_2) and equilibrium determined enzyme-substrate complex concentrations (Broholm et al., 1992; Ely et al., 1995):

$$\frac{-\mathrm{d}S_1}{E_0\mathrm{d}t} = \frac{k_1[ES_1]}{[E]+[ES_1]+[ES_2]+[ES_1S_1]+[ES_2S_2]+[ES_1S_2]+[ES_2S_1]} \tag{9}$$

$$\frac{-\mathrm{d}S_2}{E_0\mathrm{d}t} = \frac{k_2[ES_2]}{[E]+[ES_1]+[ES_2]+[ES_1S_1]+[ES_2S_2]+[ES_1S_2]+[ES_2S_1]}. \tag{10}$$

The total enzyme concentration $(E_0) = E + ES_1 + ES_2 + ES_1S_1 + ES_2S_2 + ES_1S_2 + ES_2S_1$, where the free enzyme (E) will combine with phenol (S_1) and 4-CP (S_2) to form enzyme-substrate complexes. Potential interactions between growth and nongrowth substrates include substrate inhibitions and cross-inhibitions.

The concentration of each enzyme-complex species can be further written in terms of substrate concentration and dissociation constants (e.g., $K_1 = [E][S_1]/[ES_1]$; therefore, $[ES_1] = [E][S_1]/K_1$). By substituting for the concentration of each enzyme-substrate species into Eqs. (9) and (10), and treating E_0 as cell concentration (X), the degradation rate of the growth and nongrowth

Table 2
Kinetic parameters used in modeling synchronous degradation of 4-CP and phenol

Kinetic parameter	Values	Estimated method
k_1, mg phenol/mg cell h	1.2	Phenol alone tests
k_2, mg 4-CP/mg cell h	0.15	Resting cells test
K_1, mg phenol/l	1.5	Phenol alone tests
K_{11}, mg phenol/l	250	Phenol alone tests
K_{12}, mg phenol/l	233	Phenol/4-CP tests
K_2, mg 4-CP/l	0.15	Dorn and Knackmuss (1978)
K_{22}, mg 4-CP/l	60	Resting cells tests
K_{21}, mg 4-CP/l	194	Phenol/4-CP tests

substrates is obtained in terms of substrate concentration (S_1, S_2) and the model parameters:

$$-\frac{dS_1}{dt} = \frac{\frac{k_1 X S_1}{K_1}}{1 + \frac{S_1}{K_1} + \frac{S_2}{K_2} + \frac{S_1^2}{K_1 K_{11}} + \frac{S_2^2}{K_2 K_{22}} + \frac{S_1 S_2}{K_1 K_{12}} + \frac{S_1 S_2}{K_2 K_{21}}}, \quad (11)$$

$$-\frac{dS_2}{dt} = \frac{\frac{k_2 X S_2}{K_2}}{1 + \frac{S_1}{K_1} + \frac{S_2}{K_2} + \frac{S_1^2}{K_1 K_{11}} + \frac{S_2^2}{K_2 K_{22}} + \frac{S_1 S_2}{K_1 K_{12}} + \frac{S_1 S_2}{K_2 K_{21}}}, \quad (12)$$

where K_{12} and K_{21} are the cross-substrate inhibition constants by phenol and 4-CP, respectively.

Table 2 provides the values for all parameters used in the model simulation. All the model parameters except K_{12} and K_{21} were obtained from the growth data with phenol alone and 4-CP transformation by resting cells of *Acinetobacter*. The cross-inhibitory constants (K_{12} and K_{21}) were estimated through a dynamic nonlinear optimization technique using the 4-CP transformation data in the presence of phenol shown in Fig. 11. The simulation results for the synchronous disappearance of phenol and 4-CP are shown as dash lines in Fig. 11. Excellent agreement between the model predictions and the experimental data for disappearance of phenol and 4-CP was obtained for the cases when the initial phenol:4-CP concentration ratio was 300:25 mg/l (Fig. 11). Similarly, generally good agreement was also found for an initial phenol:4-CP concentration ratio of 200:50 (data not shown).

4. Summary and conclusions

The kinetics of phenol and 4-CP biodegradation by an isolated *Acinetobacter* strain were investigated. Batch phenol degradation tests clearly demonstrated an inhibitory effect at higher phenol concentrations. Model analyses indicated that the Haldane kinetic model using experimentally determined parameter values adequately predicted phenol and cell concentrations. However, the Haldane substrate inhibition kinetics were found to be inadequate at high substrate concentrations.

4-CP degradation experiments using resting, phenol-induced *Acinetobacter* cultures indicated the likely involvement of oxygenase-mediated reactions in the transformation of 4-CP. In addition, an array of resting-cell 4-CP transformation batch experiments demonstrated several key characteristics. First, the concentration of 4-CP was immediately reduced to a lower level. The amount of the reduction was proportional to the initial amount of cell biomass used, but the exact mechanism of this initial reduction is unclear. Second, observations of residual amounts of 4-CP at the conclusion of these experiments indicated a finite transformation capacity for 4-CP by the resting cells. This is possibly due to the depletion of cell internal energy reserves. Third, decreased 4-CP transformation rates with higher initial 4-CP concentrations indicated that 4-CP inhibited its own degradation. Indeed, a Haldane model for substrate utilization using experimentally estimated parameter values was able to describe the trends in 4-CP transformation by the resting cell cultures.

Finally, when phenol and 4-CP were both present, synchronous phenol and 4-CP utilization by the *Acinetobacter* isolate was observed when the initial phenol:4-CP concentration ratio was sufficiently high (>200:50 mg/l). These data indicated that under such conditions, sufficient energy from the phenol utilization was available for 4-CP transformation. The 4-CP and phenol transformation data were described using a competitive kinetic model of cometabolism that included growth and nongrowth substrate inhibition and cross-inhibition terms. This model successfully predicted the synchronous disappearance of the phenol and 4-CP mixture.

References

Allsop, P.J., Chisti, Y., Moo-Young, M., Sullivan, G.R., 1993. Dynamics of phenol degradation by *Pseudomonas putida*. Biotechnol. Bioeng. 41, 572–580.

Alvarez-Cohen, L., McCarty, P.L., 1991. Cometabolic biotransformation model for halogenated aliphatic compounds exhibiting product toxicity. Environ. Sci. Technol. 25, 1381–1387.

Andrews, J.F., 1968. A mathematical model for continuous culture of microorganisms utilizing inhibitory substrates. Biotechnol. Bioeng. 10, 707–723.

Broholm, K., Christensen, T.H., Jensen, B.K., 1992. Modeling TCE degradation by a mixed culture of methane-oxidizing bacteria. Water Res. 26, 1177–1185.

Bouvet, P.J.M., Grimont, P.A.D., 1986. Taxonomy of the genus *Acinetobacter* with the recognition of *Acinetobacter baumannii* sp. nov., *Acinetobacter haemolyticus* sp. nov., *Acinetobacter johnsonii*. nov., and *Acinetobacter junii* sp. nov. and emended descriptions of *Acinetobacter calcoaceticus* and *Acinetobacter lwoffii*. Int. J. Syst. Bacteriol. 36, 228–240.

Chang, M.-K., Voice, T.C., Criddle, C.S., 1993. Kinetics of competitive inhibition and cometabolism in the biodegradation of benzene, toluene, and *p*-xylene by two *Pseudomonas* isolates. Biotechnol. Bioeng. 41, 1057–1065.

D'Adamo, P.D., Rozich, A.F., Gaudy, A.F., 1984. Analysis of growth data with inhibitory carbon sources. Biotechnol. Bioeng. 26, 397–402.

D'Aquino, M., Korol, S., Santini, P., Moretton, J., 1988. Biodegradation of phenolic compounds I. Improved degradation of phenol and benzoate by indigenous strains of *Acinetobacter* and *Pseudomonas*. Rev. Latinoam. Microbiol. 30, 238–288.

Dorn, E., Knackmuss, H.J., 1978. Chemical structure and biodegradability of halogenated compounds: Substituent effects on 1,2-dioxygenation of catechol. Biochem. J. 174, 85–94.

Du Preez, J.C., Toerien, D.F., Lategan, P.M., 1981. Growth parameters of *Acinetobacter calceacetious* on acetate and ethanol. Eur. J. Appl. Microbiol. Biotechnol. 13, 45–53.

Edwards, V.H., 1970. The influence of high substrate concentration on microbial kinetics. Biotechnol. Bioeng. 12, 679–712.

Ely, R.L., Williamson, K.J., Guenther, R.B., Hyman, M.R., Arp, D.J., 1995. A cometabolic kinetics model incorporating enzyme inhibition, inactivation, and recovery: I. Model development, analysis, and testing. Biotechnol. Bioeng. 46, 218–231.

Folsom, B.R., Chapman, P.J., Pritchard, P.H., 1990. Phenol and trichloroethylene degradation by *Pseudomonas cepacia* G4: kinetics and interactions between substrates. Appl. Environ. Microbiol. 56, 1279–1285.

Fox, B.G., Borneman, J.G., Wackett, L.P., Lipscomb, J.D., 1990. Haloalkene oxidation by the soluble methane monooxygenase from *Methylosinus trichosporium* OB3b: mechanistic and environmental implications. Biochem. 29, 6419–6427.

Gibson, D.T., 1968. Microbial degradation of aromatic compounds. Science 161, 1093–1097.

Hamilton, G.A., 1974. Chemical models and mechanisms for oxygenases. In: Hayaishi, O. (Ed.), Molecular Mechanisms of Oxygen Activation. Academic Press, New York.

Hill, G.A., Robinson, C.W., 1975. Substrate inhibition kinetics: phenol degradation by *Pseudomonas putida*. Biotechnol. Bioeng. 17, 1599–1615.

Kim, M.H., Hao, O.J., 1999. Cometabolic degradation of chlorophenols by *Acinetobacter* species. Water Res. 33, 562–574.

Kim, M.H., Hao, O.J., Wang, N.S., 1997. *Acinetobacter* isolates from different activated sludge processes: characteristics and neural network identification. FEMS Microbiol. Ecol. 23, 217–227.

Knackmuss, H.J., Helwig, M., 1978. Utilization and cooxidation of chlorinated phenols by *Pseudomonas* sp. B 13. Arch. Microbiol. 117, 1–7.

Loh, K.-C., Yu, Y.-G., 2000. Kinetics of carbazole degradation by *Pseudomonas putida* in presence of sodium salicylate. Water Res. 34, 4131–4138.

Okaygun, M.S., Green, L.A., Akgerman, A., 1992. Effects of consecutive pulsing of an inhibitory substrate on biodegradation kinetics. Environ. Sci. Technol. 26, 1746–1752.

Oldenhuis, R., Oedzes, J.Y., van der Waarde, J., Janssen, D.B., 1991. Kinetics of chlorinated hydrocarbon degradation by *Methylosinus trichosporium* OB3b and toxicity of trichloroethylene. Appl. Environ. Microbiol. 57, 7–14.

Pawlowsky, U., Howell, J.A., 1973. Mixed culture biooxidation of phenol. I. Determination of kinetic parameters. Biotechnol. Bioeng. 15, 889–896.

Polnisch, E., Kneifel, H., Franzke, H., Hofmann, K.H., 1992. Degradation and dehalogenation of monochlorophenols by the phenol-assimilating yeast *Candida maltose*. Biodegrad. 2, 193–199.

Rozich, A.F., Gaudy, A.F., 1985. Response of phenol-acclimated activated sludge process to quantitative shock loading. J. Water Pollut. Control Fed. 57, 795–804.

Rozich, A.F., Gaudy, A.F., D'Adamo, P.C., 1985. Selection of growth rate for activated sludge treating phenol. Water Res. 19, 481–490.

Sáez, P.B., Rittmann, B.E., 1993. Biodegradation kinetics of a mixture containing a primary substrate (phenol) and inhibitory co-metabolite (4-chlorophenol). Biodegrad. 4, 3–21.

Yang, R.D., Humphrey, A.E., 1975. Dynamic and steady state studies of phenol biodegradation in pure and mixed cultures. Biotechnol. Bioeng. 17, 1211–1235.